Article

CO Coupling Chemistry of a Terminal Mo Carbide: Sequential Addition of Proton, Hydride, and CO Releases Ethenone

Joshua A. Buss, Gwendolyn A. Bailey, Julius Oppenheim, David G. VanderVelde, William A. Goddard, and Theodor Agapie

J. Am. Chem. Soc., **Just Accepted Manuscript** • DOI: 10.1021/jacs.9b07743 • Publication Date (Web): 03 Sep 2019

CO Coupling Chemistry of a Terminal Mo Carbide: Sequential Addition of Proton, Hydride, and CO Releases Ethenone

Joshua A. Buss, Gwendolyn A. Bailey, Julius Oppenheim, David G. VanderVelde, William A. Goddard III, and Theodor Agapie

Division of Chemistry and Chemical Engineering, California Institute of Technology, 1200 E. California Blvd. MC 127-72, Pasadena, CA, USA

ABSTRACT: The mechanism originally proposed by Fischer and Tropsch for carbon monoxide (CO) hydrogenative catenation involves C–C coupling from a carbide-derived surface methylidene**.** A single molecular system capable of capturing these complex chemical steps is hitherto unknown. Herein, we demonstrate the sequential addition of proton and hydride to a terminal Mo carbide derived from CO. The resulting anionic methylidene couples with CO (1 atm.) at low-temperature (-78 °C) to release ethenone. Importantly, the synchronized delivery of two reducing equivalents and an electrophile, in the form of a hydride ($H^- = 2e^- + H^+$), promotes alkylidene formation from the carbyne precursor and enables coupling chemistry, under conditions milder than those previously described with strong one-electron reductants and electrophiles. Thermodynamic measurements bracket the hydricity and acidity requirements for promoting methylidene formation from carbide as energetically viable upon formal heterolysis of H_2. Methylidene formation prior to C–C coupling proves critical for organic product release, as evidenced by direct carbide carbonylation experiments. Spectroscopic studies, a monosilylated model system, and Quantum Mechanics computations provide insight into the mechanistic details of this reaction sequence, which serves as a rare model of the initial stages of the Fischer Tropsch synthesis.

INTRODUCTION

The Fischer-Tropsch (FT) synthesis is a well-established industrial-scale process that uses synthesis gas, a mixture of CO and H_2, as a feedstock for the generation of a broad range of catenated products.[1-5] While the variation in outputs can be versatile, it is often cost prohibitive in regards to petroleum substitution.[1-2] As efforts increase to synthesize biodiesels from renewably sourced synthesis gas,[6-7] shifting FT catalysis toward specific desirable products becomes ever more important.[7] Understanding the operative mechanism(s) of FT provides potential for rational catalyst design and, in turn, improved selectivity.[1-2, 8]

While there is little consensus as to the operative mechanism(s) of FT,[9-10] all proposals share two fundamental commonalities—CO reduction (via C–H bond formation and/or C–O cleavage) and C–C coupling. The elementary step of C–C coupling between CO and surface hydrocarbons has been studied extensively in model systems.[1,11-12,13-14] In contrast, the investigation of carbide/CO coupling remains largely underexplored. In seminal studies of carbonyl-bridged metal carbide ensembles,[15] more exposed carbides demonstrated enhanced reactivity, including C/CO coupling in the Fe_3 cluster.[16] Additional examples of C≡O cleavage and coupling have been reported, likely via carbide intermediacy, with oxophilic metals.[17-19] To our knowledge, CO coupling has yet to be demonstrated from a terminal carbide precursor, likely due to the paucity of reactive yet well-characterized examples of such motifs.[20-24]

Previous work in our group has focused on reductive C–O catenation chemistry employing one electron reductants (KC_8) and silyl electrophiles, demonstrating the deoxygenation of bound CO to a terminal carbide (**1**, Scheme 1).[25] This reactivity models the early steps proposed for FT, achieving the six-electron cleavage of CO using reducing equivalents stored in a redox non-innocent supporting ligand. C–C coupling was achieved via an isolated silyl alkylidyne complex, which, upon addition of two equiv. of strong reductant (KC_8 or naphthalenide) followed by strong electrophiles (silyl chlorides), afforded disilylketene (Scheme 1, top).[25-26]

In contrast to these relatively harsh reducing conditions, several molecular FT models have employed proton and hydride equivalents as the products of heterolytic cleavage of H_2.[27-29] Herein, we revisit CO coupling chemistry from terminal carbide **1**, the first reported example of a terminal group VI carbide bearing d-electrons. While C–C bond formation from this species is facile, it ultimately results in deleterious ligand functionalization. Sequential proton and hydride delivery convert complex **1** to a terminal methylidene via an isolated terminal methylidyne (Scheme 1, bottom). Importantly, thermochemical experiments with $NaBHPh_3$ and $[Ar_2PhPMe]Cl$ (Ar = 2,4,6-trimethoxyphenyl) provide a formal demonstration that thermodynamically H_2 can promote reduction and protonation of complex **1**, illustrating the feasibility of using proton and hydride as H_2 surrogates in carbide conversion chemistry. Addition of exogenous CO to the formed methylidene releases ketene, demonstrating the sequential formation of two C–H bonds and C/CO coupling, to yield a silicon-free, metal-free C_2O_1 organic.

Scheme 1. Mechanistically Distinct Modes of C/CO Coupling to *Free* Ketene Fragments [30]

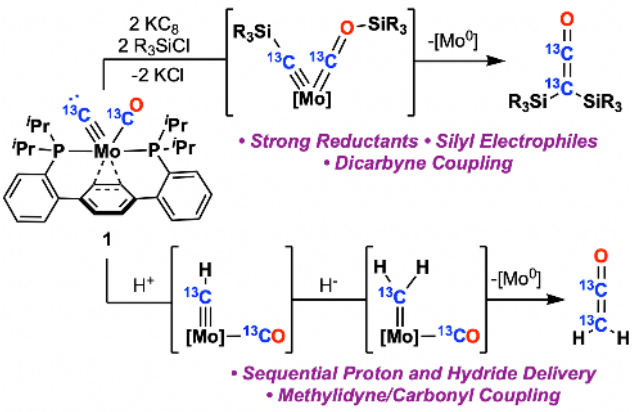

RESULTS AND DISCUSSION

Carbide/CO Coupling Reactivity

Direct carbide carbonylation represents an early bifurcation in the mechanistically complicated FT process; surface C_2 formation via carbide/CO coupling has been proposed for syngas conversion on iron foils.[31] To explore carbide/CO coupling in a well-defined system, complex **1** was treated with CO (Scheme 2).[30,32] Admission of one atmosphere (1 atm) of ^{13}CO to a THF solution of **1** at -80 °C showed no effect; however, upon warming to 25 °C, new spectral features were observed. A peculiar high-field doublet of doublets (-32.14 ppm, $^1J(P,C)$ = 118 and $^1J(C,C)$ = 103 Hz) was present in the $^{13}C\{^1H\}$ NMR spectrum, in addition to two downfield resonances. Concomitantly, two new features were observed in the $^{31}P\{^1H\}$ NMR spectrum, including a doublet of doublet of doublets (37.64 ppm, $^1J(P,C)$ = 118.1 Hz, $^2J(P,C)$ = 33.2 Hz, & $^3J(P,P)$ = 4.2 Hz) displaying strong scalar coupling to the high-field carbon. The large P–C and C–C spin-spin coupling constants, in addition to the broken symmetry of the terphenyl diphosphine (**P2**) ligand, are most consistent with formation of a Mo-bound phosphoranylideneketene, **2**.

Scheme 2. CO Coupling Chemistry of Terminal Molybdenum Carbides[a]

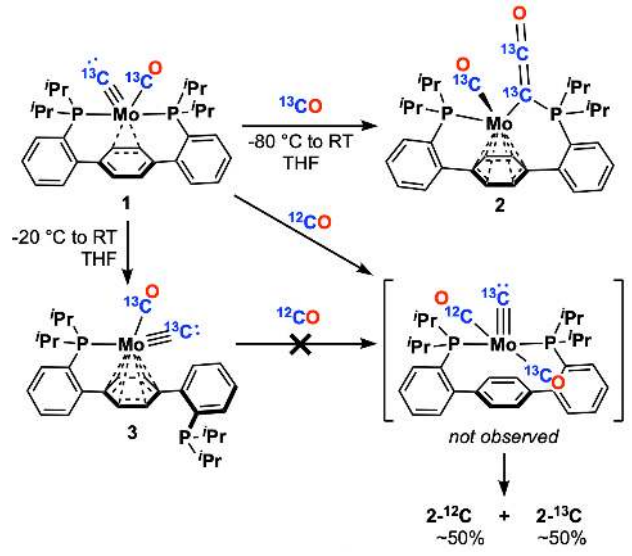

[a] Carbide **1** was synthesized cleanly *in situ* via deprotonation of P2Mo(CH)(CO)(Cl) **4** with benzyl potassium. For more details, see the Supporting Information.

A single-crystal X-ray diffraction (XRD) study of **2** confirmed the proposed assignment (Figure 1). The short C31–C32 bond length and wide C31–C32-O1 angle (1.2885(11) Å and 179.01°, respectively) support assignment of the η^1-C(P)=C=O bonding motif.[33] Mo engages the central arene in an η^6 fashion, to stabilize the low-valent metal center resulting from C–C coupling. Transition metal-bound phosphoranylidene ketenes, relatively rare motifs, are generally prepared via reaction of a metal precursor with preformed ketene, R_3PCCO.[34] In one example, the P–C linkage was formed at the metal center, from cleavage of carbon suboxide.[35] Complex **2** therefore represents the first example of such a motif in which both the P–C and C–C bonds were formed at the metal center.

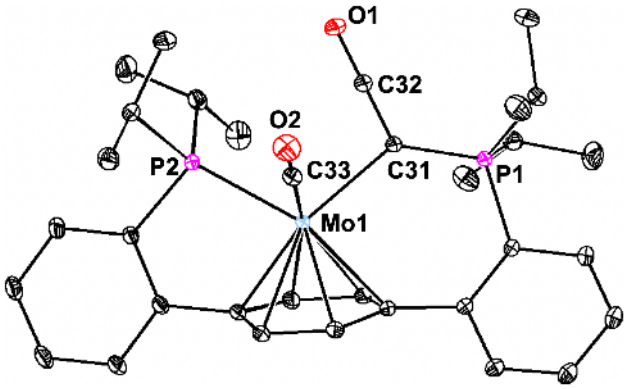

Figure 1. Solid-state structure of **2**. Thermal anisotropic displacement ellipsoids are shown at the 50% probability level. H-atoms are omitted. Selected bond distances [Å] and angles [°]: P1–C31 1.7144(11), C31–C32 1.2885(11), C32–O1 1.1865(10), Mo1–C31 2.2899(16), Mo1–C33 1.9563(12), C33–O2 1.1693(10), C31–C32–O1 179.01(8), P1–C31–Mo1 130.73(5).

We hypothesized that CO binding could induce C–C bond formation[36-37] in **1** via a putative dicarbonyl carbide intermediate (Scheme 2). Labeling experiments were conducted to explore this process. Addition of ^{12}CO to **1** results in a 50:50 mixture of isotopes at the phosphoranylideneketene α-carbon (Figure 2). Likewise, the $^{31}P\{^1H\}$ NMR spectrum displays a broad resonance for the Mo-bound phosphine arm comprised of an overlapping doublet of doublets and doublet, the former split by partial (*ca.* 50%) ^{13}C enrichment at the carbonyl carbon. Taken together, these data are consistent with an intramolecular coupling pathway from a proposed dicarbonyl carbide complex. This process contrasts the ostensibly similar cleavage and coupling of CO by $Ta(silox)_3$,[38] which, through a series of detailed mechanistic studies, was shown to form the C–C bond prior to the first deoxygenation event, *en route* to a ditantalum dicarbide ($(silox)_3Ta{\equiv}CC{\equiv}Ta(silox)_3$).[39] Related transformations starting from alkylidyne carbonyl complexes, with addition of phosphines leading to the assembly of *neutral* PC(R)=C=O ligands, have also been reported.[40-43] Combined, these molecular systems represent complementary precedents for potential elementary steps in the early stages of the FT synthesis.

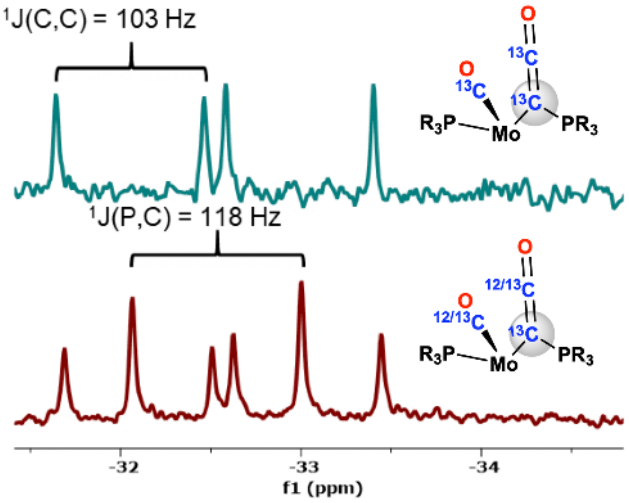

Figure 2. High-field partial $^{13}C\{^1H\}$ NMR spectra of **2** generated under ^{13}CO (top) and ^{12}CO (bottom) showing splittings for the phosphoranylidene ^{13}C nucleus circled in grey.

Recognizing that carbide **1** need not bind an additional molecule of CO to form a ketenylidene, it was slowly warmed to RT. While this results in a composite mixture of largely intractable species,[25] one of these complexes proved highly soluble. Extraction of the crude residue with hexamethyldisiloxane afforded a deep purple solution, which upon standing at -35 °C, precipitated **3** as a purple powder. While single crystals of **3** have proven elusive, the structure can be confidently inferred from multinuclear NMR spectroscopy. A diagnostic carbidic $^{13}C\{^1H\}$ resonance is observed at 569.86 ppm, further downfield shifted from that of **1**. Two distinct features in the $^{31}P\{^1H\}$ NMR spectrum at 91.44 and -4.08 ppm support an arm-on arm-off binding mode for the **P2** ligand, and four upfield aromatic ^1H shifts corroborate an η^6 metal-arene interaction. Addition of 1 atm of CO to solutions of **3** likewise did not afford the coupled product **2**, however. Instead, an intractable mixture is formed, together with free **P2**, reflecting additional, deleterious pathways that are enabled by dissociation of the second phosphine arm.

Carbide Protonation, Hydride Transfer, and Methylidene/CO Coupling

Toward modeling the proposed role of surface hydrides in FT, and ultimately forming C–H bonds, carbide protonation was targeted.[21, 44] Addition of Et_3NHCl to a -78 °C THF solution of **1** results in formation of a new compound upon warming to room temperature. A single resonance between 3.5 and 6.5 ppm is observed in the ^1H NMR spectrum, a doublet of triplets centered at 5.06 ppm (^1J(C,H) = 147.8 Hz, ^3J(P,H) = 3.1 Hz), with a relative integration of one. This suggests both a terminal methylidyne[20, 24, 45-51] and a five-coordinate *pseudo*-square pyramidal structure, as in **4**, without metal-arene interactions (*vide infra*; Scheme 3). The $^{31}P\{^1H\}$ and $^{13}C\{^1H\}$ NMR data further corroborate the proposed assignment of **4**, with a doublet of doublets at δ_P 40.21 ppm (^2J(C,P) = 18.6 and 10.2 Hz) and a characteristic methylidyne resonance at δ_C 281.19 ppm, respectively.[45, 51]

Scheme 3. Sequential Proton and Hydride Addition *en route* to Ketene Formation [a]

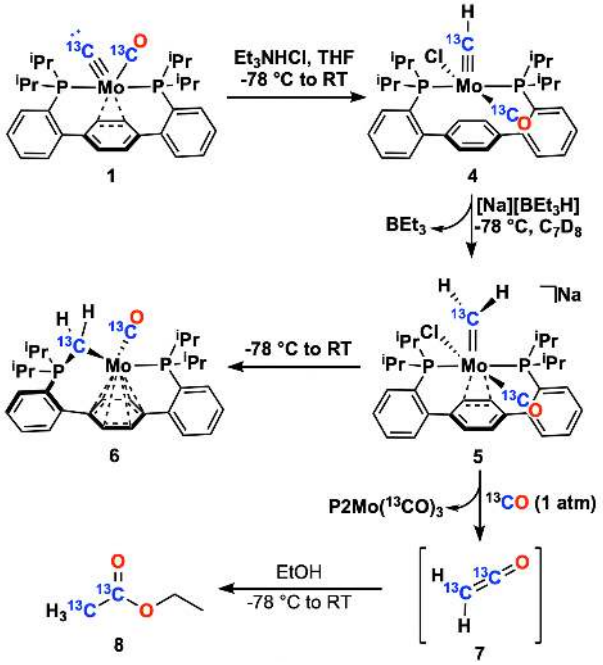

[a] Carbide **1** was synthesized cleanly *in situ* via deprotonation of P2Mo(CH)(CO)(Cl) **4** with benzyl potassium. For more details, see the Supporting Information.

Gratifyingly, **4** is thermally stable, facilitating both its use for reaction chemistry and permitting growth of single crystals. A single-crystal XRD study corroborates the structure inferred from spectroscopy (Figure 3). The Mo center sits above the central arene ring at a distance of 2.749 Å, suggesting negligible metal arene interaction. The Mo≡CH distance is appropriately short (1.764(2) Å) but slightly longer than that in a structurally characterized Mo(VI) methylidyne (1.702(5) Å),[44] likely a manifestation of the more-reduced metal center.

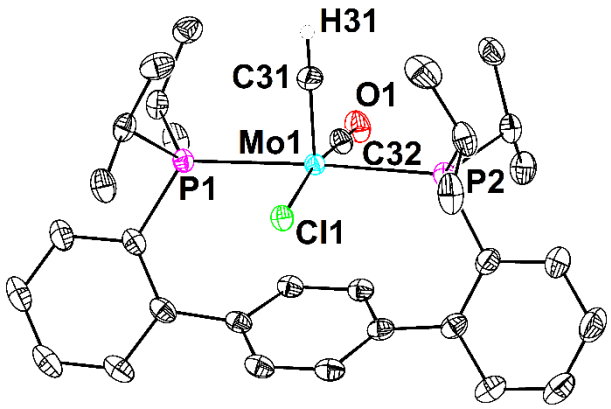

Figure 3. Solid-state structure of **4**. Thermal anisotropic displacement ellipsoids are shown at the 50% probability level. H-atoms are omitted, except for the methylidyne proton, which was refined freely. Selected bond distances [Å] and angles [°]: Mo1–C31 1.764(2), Mo1–C32 1.930(4), O1–C32 1.197(6).

Hydride addition to both terminal[21] and bridging[52] methylidyne ligands has precedent, and we sought to target this reactivity, considering proton and hydride as a crude surrogate for H_2 (*vide infra*). $NaBEt_3H$ was added to a C_7D_8

solution of **4** at -78 °C. Mixing the reagents immediately resulted in a color change to dark brown, and VT NMR spectroscopy showed signals in the $^{31}P\{^{1}H\}$ (s, 52.07 ppm), $^{13}C\{^{1}H\}$ (br s, 296.91 and br s, 237.52 ppm), and ^{1}H (15.03, d, ^{1}J(C,H) = 114.90 Hz and 13.27, d, ^{1}J(C,H) = 142.7 Hz) spectra, in line with formation of methylidene **5** (Scheme 3).[21] Warming the sample to 0 °C, showed quantitative conversion to a new asymmetric complex with a triplet of doublets (84.68 ppm, $^{2}J(P,C_{CO})$ = 15.5 & $^{2}J(P,C_{CH2})$ = 6.0 Hz) and doublet of doublets (47.41 ppm, $^{1}J(P,C_{CH2})$ = 21.9 ppm & $^{2}J(P,C_{CO})$ = 17.0 Hz) in the $^{31}P\{^{1}H\}$ NMR spectrum. The $^{13}C\{^{1}H\}$ NMR spectrum likewise showed two signals, a broad doublet of triplets centered at 251.88 ppm ($^{2}J(C_{CO},P)$ = 15.3 & $^{2}J(C_{CO},C_{CH2})$ = 2.2 Hz) and an extremely high-field resonance at -34.87 ppm (ddd, $^{1}J(C_{CH2},P)$ = 21.8, $^{2}J(C_{CH2},P)$ = 6.2 Hz & $^{2}J(C_{CH2},C_{CO})$ = 2.2 Hz). The high-field chemical shift in the $^{13}C\{^{1}H\}$ NMR spectrum[49] and the C_1 symmetry are consistent with P–C bond formation, giving **6**,[53-54] unexpectedly suggesting some electrophilic carbene character in electron-rich, anion **5**.[53-55] The small $^{1}J(P,C_{CH2})$ spin-spin coupling[56] observed for **6** is consistent with phosphonium ylide complexation to transition metal centers; ligation results in rehybridization—C(sp^2) to C(sp^3)—that is reflected in the smaller one-bond scalar coupling constant.[57] The structure of **6** was confirmed in a single-crystal XRD study, which corroborated the assignment of the η^1-C-bound ylide moiety (see the SI).

We hypothesized that similarly to the effect observed for carbide/CO coupling, methylidene/CO coupling may be favored by addition of exogenous CO, either via direct CO attack[58] or coordination to Mo. Placing a -78 °C solution of *in situ* generated **5** under a ^{13}CO atmosphere resulted in a gradual color change to bright orange, as the gas diffused down the sample (Scheme 3). The $^{13}C\{^{1}H\}$ NMR spectrum at -78 °C, showed both free ^{13}CO and three resonances in the metal-bound region—the CO signals of previously characterized **P2Mo(^{13}CO)$_3$**.[59]

Anticipating that zero-valent Mo was indicative of a C–C coupling process, identification of ethenone by $^{13}C\{^{1}H\}$ NMR spectroscopy was attempted. The diagnostic signals for free ketene (^{13}C δ = 193.7 and 2.7 ppm)[60] were absent, but coupling doublets at 154.69 and 83.90 ppm (^{1}J(C,C) = 76.1 Hz) were observed, attributed to a putative ethenone-triethyl borane adduct.[61] While further efforts to detect free ethenone (**7**) were unsuccessful, ketene trapping with ethanol has precedent, giving stable and easily detectable ethyl acetate (EtOAc).[60, 62] Forming **5** at low temperature, adding ^{13}CO, and condensing EtOH into the reaction tube afforded EtOAc-$^{13}C_2$, **8**, unequivocally demonstrating the generation and ejection of parent ketene (Scheme 3). Alkylidene carbonylation has been demonstrated on a variety of molecular scaffolds,[13] but often requires CO overpressures,[58, 63-65] proceeds from activated Fischer carbene complexes,[13, 66-68] or occurs at bridging alkylidene ligands.[69-70] Rarely is this coupling achieved at monometallic complexes with carbene fragments derived from CO.[67, 71-73]

Isotopic labeling studies were conducted in which ^{12}CO was added to **5**. Mixed isotopolog **P2Mo($^{12/13}$CO)$_3$** was formed, consistent with either i) rapid exchange of the ^{13}CO ligand in **5** with free ^{12}CO and on-metal C–C bond formation or ii) ^{12}CO binding and C–C coupling preceding from a methylidene dicarbonyl complex. We favor the latter, given that coordination to Mo facilitates C–C coupling chemistry in the related carbide/CO chemistry described above.

Reactivity of a Silylcarbyne Model System

Expecting that similar C/CO coupling chemistry would be achieved from silyl carbyne **9**, affording a more stable organic product, a related reactivity sequence was explored with this silyl model system (Scheme 4). Low-temperature addition of $NaBEt_3H$ to a C_7D_8 solution of alkylidyne **9** and subsequent warming to -20 °C resulted in the gradual formation of a new species demarcated by a $^{31}P\{^{1}H\}$ resonance at 48.53 ppm and low-field doublet in the ^{1}H NMR spectrum (δ = 15.79 ppm, ^{1}J(C,H) = 121.7 Hz). Such a signal could be consistent with either formyl generation,[74-77] via CO insertion into an intermediate Mo hydride (a process that is facilitated by borane Lewis acids),[29, 78-80] or hydride attack at the carbyne to give a silyl alkylidene. The ^{13}C NMR spectrum was more informative, displaying a broad doublet at 315.09 ppm (^{1}J(C,H) = 121.7 Hz) and a broad singlet at 251.83 ppm (Figure S28). C–H coupling to the more downfield resonance is suggestive of a carbene/carbonyl isomer rather than the alternative carbyne/formyl complex. 2D $^{1}H/^{13}C$ correlation experiments further disambiguated the structure (Figure S29), with strong HMBC cross peaks between the H-bound carbon atom and the $SiMe_3$ methyl protons. These data point to hydrogen transfer to the alkylidyne carbon,[21, 81-83] affording silyl carbene **10**, in analogy to the reactivity observed for parent methylidyne **4** (*vide supra*).

Scheme 4 Hydride-Initiated C–C Coupling.

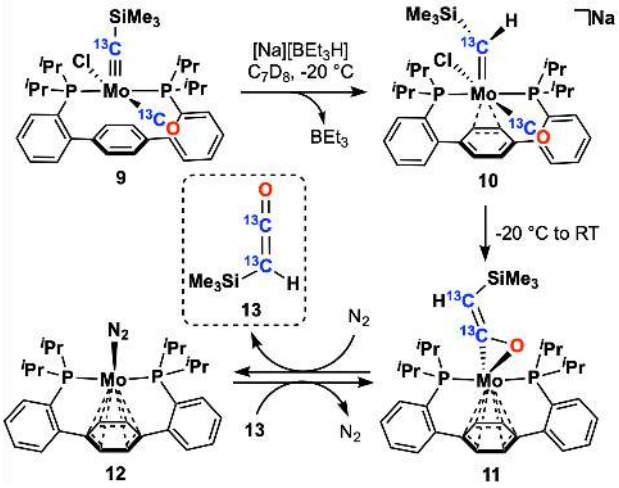

While **10** was the major species observed at -20 °C, it proved transient, slowly reacting further to give a mixture of two Mo complexes with a doublet and singlet in the ^{31}P NMR spectrum at 58.38 and 76.24 ppm, respectively. The latter corresponds to previously characterized Mo^0-N_2 adduct **12**,[59, 84] demonstrating loss of the carbon-based ligands, presumably via C–C coupling. The isotopically enriched ^{13}C signals at 84.76 and 191.35 ppm showed strong scalar coupling (^{1}J(C,C) = 69.7 Hz), the latter split into a doublet of triplets (^{2}J(C,P) = 26.3 Hz) by the trans-spanning phosphines of the **P2** ancillary ligand. This spectral signature is consistent with C–C bond formation affording the trimethylsilyl ketene complex **11**. Interestingly, in this case, CO addition is not requisite for C–C coupling.

The assignment of **11** was further supported via independent synthesis.[85] Anticipating that the observed mixture of **11** and **12** resulted from a ligand substitution equilibrium between the isoelectronic Mo^0 adducts, a C_6D_6 solution of **12** was treated with trimethylsilyl ketene.[86] While only starting material was observed under an N_2 atmosphere, degassing the reaction mixture resulted in significant conversion to **11**, as evidenced by $^{31}P\{^1H\}$ NMR spectroscopy. The N_2/ketene exchange was borne out in the hydride-initiated C–C coupling chemistry; in addition to the coupling doublets of the bound ketene, a pair of doublets at 192.48 and 60.28 ppm (^1J(C,C) = 73.5 Hz) were observed in the ^{13}C NMR spectrum, corresponding to the metal-free C_2 fragment.[61]

An XRD study of single crystals of **11** grown from slow evaporation of liquid butane confirmed the inferred η^2-CO ketene assignment (Figure 4), with comparable O1-C31 (1.2799(12) Å) and C31-C32 (1.3536(14) Å) distances.[87-89] η^2-CC ketene adducts are known,[90-92] but the O-bound form is often thermodynamically favored.[90] Contrasting the structure of **9**,[25] As in the structure of **2** above, the central arene is engaged in η^6 coordination to Mo, consistent with the more reduced Mo center formed on C–C coupling.

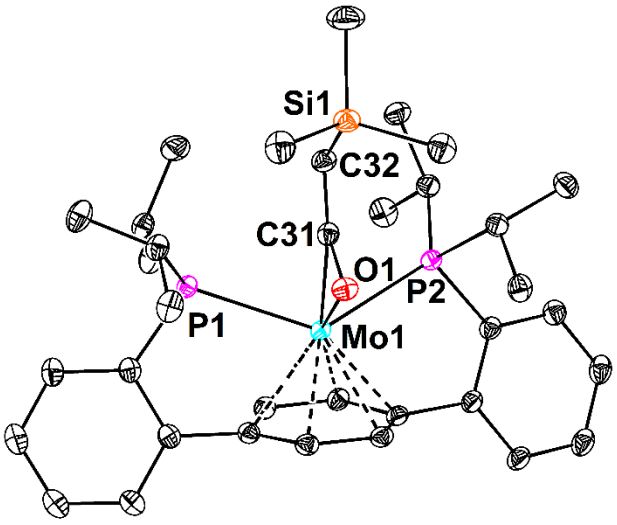

Figure 4. Solid-state structure of **11**. Thermal anisotropic displacement ellipsoids are shown at the 50% probability level. H-atoms are omitted for clarity. Selected bond distances [Å] and angles [°]: Mo1–O1 2.1858(7), Mo1–C31 2.1629(10), Mo1–C_{arene} (ave.) 2.2599(9), O1–C31 1.2799(12), C31–C32 1.3536(14), ∠O1-C31-C32 132.32(9).

Quantum Mechanics Computations

Akin to the sequential addition of potassium graphite and silyl electrophile to alkylidyne **9**,[25-26] $NaBEt_3H$ proved proficient for enacting the reductive coupling of silyl carbyne with CO. The latter reactivity manifold, preceding through a carbene intermediate (**10**) rather than a dicarbyne complex, is accessible under much milder conditions and shows equal efficacy in C–C coupling. Given the facility with which the catenation proceeds, Quantum Mechanics computation (using the M06-2X flavor of Density Functional Theory)[93] was employed to interrogate the electronic structure requirements in the critical bond-forming step. The optimized structure following hydride addition to **9** resembles silyl alkylidene **10**,[94] in agreement with experiment; however, a close contact between Na^+ and the Cl ligand is observed in addition to borane binding to the carbonyl (Figure S42). [95] The HOMO of this complex, with d_{xz} parentage, is dominated by a π-bonding interaction with CO (**10•BEt$_3$**, Figure 5, inset). As the C–C distance contracts, the alkylidene ligand rotates, directing the Mo–CSi π-system towards CO (**^{1}X**, Figure 5). This geometry has a d_{yz} HOMO stabilized by M-arene backbonding. With further C–C shortening, the ground state crosses to a triplet, resulting from electron promotion from the d_{yz} (Mo– arene π) to the d_{xz} (Mo–CSi π^*) and representing cleavage of the Mo–C π-bond (**^{1}X** to **^{3}X**, Figure 5, right insets). This alkylidene activation process, with significant electron density localization on the carbon, is facilitated by the proximal Na^+ ion, without which a low-energy pathway could not be identified. Bond formation is additionally assisted by borane coordination, stabilizing the oxygen lone pair as electron density is transferred to CO.[95] The direct impact of the Lewis acids Na^+ and BH_3 on this C–C coupling process is particularly notable. While BEt_3 has no direct relevance to FT, there is precedent for both Lewis acidic promoters in FT catalysis[10] and selectivity perturbations resulting from alkali metal cation addition in electrochemical CO[96-97] reduction. Our computations highlight in a well-defined molecular system the necessity of these interactions for coupling chemistry resulting in ketene.

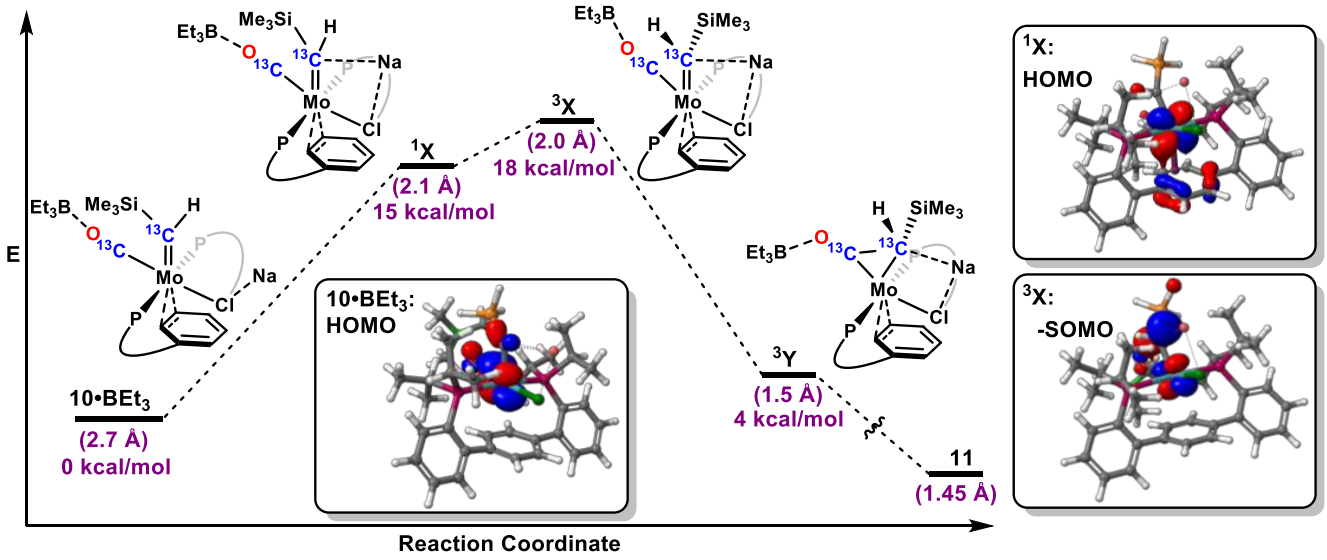

Figure 5. Potential Energy Landscape for C–C Bond Formation. Truncated transition state structures, computed C–C bond distances, and energies (relative to **10**•BEt_3) are provided. The insets depict key molecular orbitals (0.05 eÅ^{-3} isosurfaces) involved in bond-breaking and making steps.

Thermochemistry of Proton and Hydride Transfer to Carbide 1

Thus far, a moderate acid (Et_3NHCl, pK_a = 14.9 in THF)[98] and a strong hydride donor ($NaBHEt_3$, $\Delta G°_{H^-}$ = 26 kcal/mol in MeCN[99]) have been described in the reaction chemistry for the formation of ethenone from **1**. These reagents are only a crude surrogate for H_2, as the free energy of hydrogen formation is favorable by *ca.* 25 kcal/mol, considering the reaction free energy of H_2 heterolysis in MeCN.[100] Given the basicity of related Mo(VI) and W(VI) carbide complexes (Mo(≡CH)(NRAr)$_3$, pK_a ~ 30 kcal/mol in THF;[20] W(≡CH)(CO)$_2$(Tp*), pK_a = 28.7 kcal/mol in THF[21]), we anticipated that weaker acids could be employed to access methylidyne **4**.

Further protonation studies assessed the basicity of carbide **1**, and supported a pK_a (Cl) for methylidyne **4** of ≥ 33.[101] Treatment of carbide **1** with the phosphazene base P2Et•HCl (Scheme 5; pK_a 26.6 in THF[102]) resulted in quantitative conversion to methylidyne **4**, with observation of the expected conjugate base P_2Et at 15.1 ppm in the $^{31}P\{^1H\}$ NMR spectrum. Reaction with the weaker acid [Ar_2PhPMe]Cl (Ar = 2,4,6-trimethoxyphenyl; pK_a 33.5 in THF[102]) likewise furnished methylidyne **4**, along with a new species, **4'**, whose NMR signature mirrored that of **4**, suggesting a closely related isomer. Most diagnostic was a ^{31}P chemical shift at 41.81 ppm, shifted only *ca.* 1.5 ppm downfield from **4**, and a diagnostic ^{13}C resonance at 267.8 ppm, which correlated by HMQC analysis to a triplet in the ^1H NMR spectrum at 2.64 ppm for the methylidyne proton (^3J(H,P)= 3.8 Hz). Independent synthesis, together with a single-crystal XRD study, confirmed **4'** to be an isomer of **4** in which the methylidyne is oriented *cis* with respect to the central arene (Figure 6). As in the previously reported cis silylcarbyne isomer,[26] the *cis* methylidyne isomer adopts a *pseudo*-octahedral geometry with a clear η^2-arene interaction *trans* to CO. The Mo–C31 distances are similar between the two isomers (*cis*/*trans* 1.781 Å vs 1.764(2), respectively), and both are consistent with a Mo-C triple bond.

The conjugate ylide $Ar_2PhP{=}CH_2$ was not detected, however (δ_P 7.00 ppm). Instead, a new peak in the ^{31}P NMR at 7.4 ppm was observed, together with free **P2** (δ_P –3.45 ppm), suggesting displacement of **P2** by ylide in the formed methylidyne complex. Competing decomposition of the carbide complex by other pathways, however, cannot be strictly ruled out. Taken together, these protonation studies suggest a lower limit of 33 for the pK_a (Cl) of methylidyne **4**, roughly three orders of magnitude higher than the closest previously reported comparator, Mo(≡CH)(NRAr)$_3$.[20] The higher effective basicity of carbide **1** may reflect diminished π-donation from the carbide ligand in this more electron-rich, formally Mo(IV), complex, and/or the favored energetics of chloride binding to Mo.

Scheme 5. Protonation studies of carbide 1.[a, b]

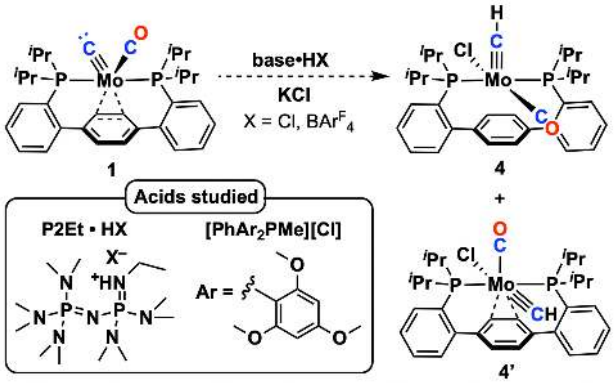

[a] pK_a values of HCl salts in THF: P2Et•HCl, 26.6;[98] [$PhAr_2PMe$][Cl], 33.5.[102] [b] Carbide **1** was synthesized cleanly in situ via deprotonation of P2Mo(CH)(CO)(Cl) **4** with benzyl potassium. For more details, see the Supporting Information.

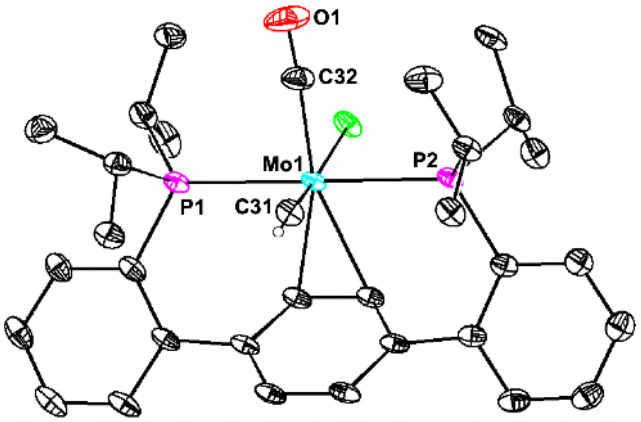

Figure 6. Solid-state structure of **4'**. Thermal anisotropic displacement ellipsoids are shown at the 50% probability level. H-atoms are omitted for clarity, except the methylidyne proton. Selected bond distances [Å] and angles [°]: Mo1–C31 1.781(2), Mo1–C32 1.972(2), O1–C32 1.155(2).

To gain insight into the hydride affinity of methylidyne **4**, weaker hydride sources were employed. Hydride transfer was complete using $NaBHPh_3$ ($\Delta G°_{H-}$ = 36 in MeCN[99]), as judged by the quantitative formation of **6** upon warming the reaction to RT. However, in a variable temperature NMR study, methylidene **5** was not observed on maintaining the reaction at –78 °C. Instead, observation of **5** necessitated warming to *ca.* –30 °C, consistent with a higher activation energy of hydride transfer from the bulkier borohydride. Up to equal proportions of **5** and **4** were observed at –20 °C, suggesting that the hydride affinity of methylidyne **4** is at least comparable to that of $NaBHPh_3$. Competing conversion of **5** to **6** occurred at these temperatures; however, preventing extraction of the exact thermodynamic parameters.

Addition of $NaBHPh_3$ at -78 °C, followed by reaction with CO (1 atm), likewise furnished **P2Mo(CO)$_3$** on warming to RT, as expected based on the thermodynamic favorability of conversion from **5** described above. A small peak assigned to **5** was apparent only at intermediate temperatures (0 °C), again consistent with the higher activation barrier using $NaBHPh_3$.

Reconsidering the relevance to H_2 splitting, the pK_a of $[Ar_2PhPMe]Cl$ and hydricity of $NaBHPh_3$ suggest that a reaction between carbide **1** and H_2 is thermodynamically downhill by at least 5 kcal / mol (Scheme 6).[103] These experiments therefore constitute a thermochemical demonstration that H_2 is a suitable source of protons and hydrides in the studied system. However, warming a THF solution of **1** under 1 atm H_2 showed only slight conversion to **3**. Direct reaction of carbides with H_2 therefore appears to be kinetically disfavored.[104] Cleavage of H_2—either heterolytically or on a surface—may be important to reaction with carbide and subsequent enabling of C–C coupling reactivity. This is in contrast to the reactivity of transition metal imides and carbenes, for which direct activation of R–H bonds (R = C, H) is kinetically allowed.[105-107]

Scheme 6. Thermochemical Cycle Evaluating Relevance to Syngas Chemistry

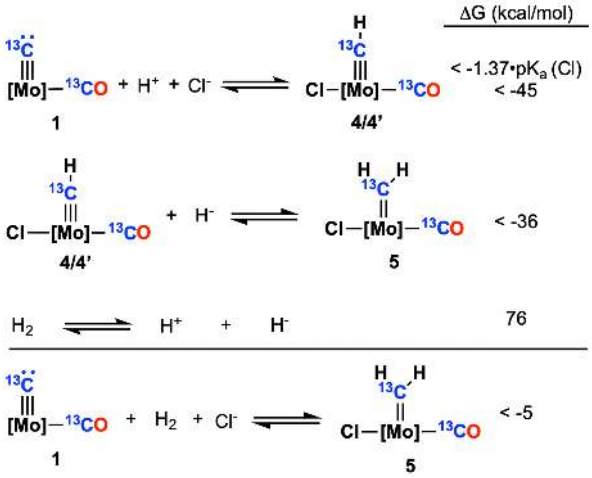

CONCLUSION

In summary, a terminal Mo carbide complex has been demonstrated to undergo direct carbonylation, in conjunction with ligand functionalization, affording a phosphoranylideneketene complex. Carbide protonation provides a thermally stable methylidyne carbonyl complex, which, upon sequential treatment with hydride and CO, induces C–C coupling. Experimental and Quantum Mechanics computational interrogation of reactions between the silyl alkylidyne congener and hydride suggest that this C–C bond formation differs from the mechanism established for stepwise reduction/electrophile addition, proceeding through carbene carbonyl intermediates rather than dicarbynes.

Notably, this reaction sequence models, with high fidelity, the proposed mechanism of FT: surrogates of H_2 react with a terminal carbide (**1**) to afford a reactive methylidene (**5**) (*cf.* **B** – **F**, Figure 7). This methylidene is the precursor to C–C bond formation, coupling with CO to give ketene. These steps provide valuable precedent for the reactivity proposed for the heterogenous FT process, mimicking the multi-electron C–C coupling reactivity postulated following C–O scission at a well-defined monometallic Mo carbide complex. Critically, the use of hydride as a FT relevant two-electron reductant provides an efficient strategy to accomplish C–C coupling and C–H bond formation. The reaction of the **1** with weak acid and hydride sources (the products of formal H_2 heterolytic cleavage) to access a methylidene contrasts the lack of reactivity observed when treated with H_2 directly, highlighting the need for pre-activation to achieve productive carbide hydrogenation in either the present molecular model system or via cleavage on the catalyst surface in FT.

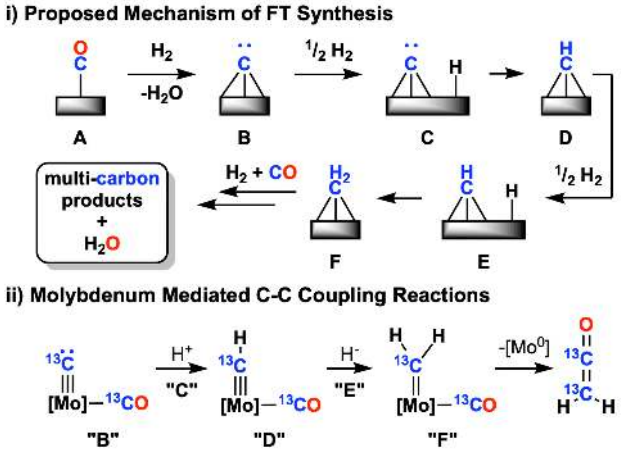

Figure 7. i) Schematic representation of the early steps of Fischer-Tropsch synthesis. **ii)** Molecular Mo Complexes Modeling C/CO Coupling to Metal-Free Organics.

ASSOCIATED CONTENT

Supporting Information

Detailed experimental procedures, full characterization, crystallographic details (CIF), and spectroscopic data. This material is available free of charge via the Internet at http://pubs.acs.org.

AUTHOR INFORMATION

Corresponding Author

*E-mail: agapie@caltech.edu

Notes

The authors declare no competing financial interests.

ACKNOWLEDGMENT

We thank Larry Henling and Mike Takase for invaluable crystallographic assistance. J.A.B. is grateful for an NSF graduate research fellowship, G.A.B. for NSERC and Resnick Sustainability Institute fellowships, and J.O. for an Ernest H. Swift Summer Undergraduate Research Fellowship. We thank the NSF (CHE-1800501), the Dow Next Generation Education Fund (instrumentation), and Caltech for funding. The computational studies were supported by the NSF (CBET-1805022).

REFERENCES

1. West, N. M.; Miller, A. J. M.; Labinger, J. A.; Bercaw, J. E. Homogeneous syngas conversion. *Coord. Chem. Rev.* **2011,** *255* (7), 881-898.
2. Herrmann, W. A. Organometallic Aspects of the Fischer-Tropsch Synthesis. *Angew. Chem. Int. Ed. Engl.* **1982,** *21* (2), 117-130.
3. Snel, R. Olefins from Syngas. *Catalysis Reviews* **1987,** *29* (4), 361-445.
4. Torres Galvis, H. M.; Bitter, J. H.; Khare, C. B.; Ruitenbeek, M.; Dugulan, A. I.; de Jong, K. P. Supported Iron Nanoparticles as Catalysts for Sustainable Production of Lower Olefins. *Science* **2012,** *335* (6070), 835-838.
5. Bao, J.; Yang, G.; Yoneyama, Y.; Tsubaki, N. Significant Advances in C1 Catalysis: Highly Efficient Catalysts and Catalytic Reactions. *ACS Catal.* **2019**, 3026-3053.
6. Ail, S. S.; Dasappa, S. Biomass to liquid transportation fuel via Fischer Tropsch synthesis – Technology review and current scenario. *Renewable and Sustainable Energy Rev.* **2016,** *58*, 267-286.
7. Zhang, X. Essential scientific mapping of the value chain of thermochemically converted second-generation bio-fuels. *Green Chem.* **2016,** *18* (19), 5086-5117.
8. Jiao, F.; Li, J.; Pan, X.; Xiao, J.; Li, H.; Ma, H.; Wei, M.; Pan, Y.; Zhou, Z.; Li, M.; Miao, S.; Li, J.; Zhu, Y.; Xiao, D.; He, T.; Yang, J.; Qi, F.; Fu, Q.; Bao, X. Selective conversion of syngas to light olefins. *Science* **2016,** *351* (6277), 1065.
9. Muetterties, E. L.; Stein, J. Mechanistic features of catalytic carbon monoxide hydrogenation reactions. *Chem. Rev.* **1979,** *79* (6), 479-490.
10. Maitlis, P. M.; Zanotti, V. The role of electrophilic species in the Fischer–Tropsch reaction. *Chem. Commun.* **2009,** (13), 1619-1634.
11. Mayr, A.; Hoffmeister, H., Recent Advances in the Chemistry of Metal-Carbon Triple Bonds. In *Adv. Organomet. Chem.*, Stone, F. G. A.; West, R., Eds. Academic Press: San Diego, 1991; Vol. 32, pp 227-324.
12. Geoffroy, G. L.; Bassner, S. L., Interaction of Ketenes with Organometaliic Compounds: Ketene, Ketenyl, and Ketenylidene Complexes. In *Adv. Organomet. Chem.*, Stone, F. G. A.; West, R., Eds. Academic Press: San Diego, 1988; Vol. 28, pp 1-83.
13. Zhang, Z.; Zhang, Y.; Wang, J. Carbonylation of Metal Carbene with Carbon Monoxide: Generation of Ketene. *ACS Catal.* **2011,** *1* (11), 1621-1630.
14. In several recent noteworthy examples, the deoxygenation and reductive cleavage of CO has been extended beyond transition metal systems to the main group. See, for example: (a) Wang, Y.; Kostenko, A.; Hadlington, T. J.; Luecke, M.-P.; Yao, S.; Driess, M. Silicon-Mediated Selective Homo- and Heterocoupling of Carbon Monoxide. *J. Am. Chem. Soc.* **2019**, *141*, 626-634. (b) Majumdar, M.; Omlor, I.; Yildiz, C. B.; Azizoglu, A.; Huch, V.; Scheschkewitz, D. Reductive Cleavage of Carbon Monoxide by a Disilenide. *Angew. Chem. Int. Ed.* **2015**, *54*, 8746-8750. (c) Arrowsmith, M.; Böhnke, J.; Braunschweig, H.; Celik, M. A. Reactivity of a Dihydrodiborene with CO: Coordination, Insertion, Cleavage, and Spontaneous Formation of a Cyclic Alkyne. *Angew. Chem. Int. Ed.* **2017**, *56*, 14287-14292.
15. Shriver, D. F.; Sailor, M. J. Transformations of carbon monoxide and related ligands on metal ensembles. *Acc. Chem. Res.* **1988,** *21* (10), 374-379.
16. Kolis, J. W.; Holt, E. M.; Drezdzon, M.; Whitmire, K. H.; Shriver, D. F. A reactive three-metal carbide cluster precursor, $[Fe_3(CO)_9(CCO)]_2$. *J. Am. Chem. Soc.* **1982,** *104* (22), 6134-6135.
17. Calderazzo, F.; Englert, U.; Guarini, A.; Marchetti, F.; Pampaloni, G.; Segre, A. $[Zr_3Cp_2(O_2CNiPr_2)_6(\mu\text{-}O)(\mu\text{-}CCO)]$, the First Crystallographically Established Ketenylidene Complex; A Model for CO Reductive Cleavage on Metal Surfaces. *Angew. Chem. Int. Ed. Engl.* **1994,** *33* (11), 1188-1189.
18. Evans, W. J.; Grate, J. W.; Hughes, L. A.; Zhang, H.; Atwood, J. L. Reductive homologation of carbon monoxide to a ketenecarboxylate by a low-valent organolanthanide complex: synthesis and x-ray crystal structure of

[$(C_5Me_5)_4Sm_2(O_2CCCO)(THF)]_2$. *J. Am. Chem. Soc.* **1985,** *107* (12), 3728-3730.

19. Calderazzo, F.; Englert, U.; Guarini, A.; Marchetti, F.; Pampaloni, G.; Segre, A.; Tripepi, G. Zirconium(II)- and Hafnium(II)-Assisted Reductive Coupling of Coordinated Carbonyl Groups Leading to Ketenylidene Complexes of Zirconium(IV) and Hafnium(IV). *Chem. Eur. J.* **1996,** *2* (4), 412-419.

20. Peters, J. C.; Odom, A. L.; Cummins, C. C. A terminal molybdenum carbide prepared by methylidyne deprotonation. *Chem. Commun.* **1997,** (20), 1995-1996.

21. Enriquez, A. E.; White, P. S.; Templeton, J. L. Reactions of an Amphoteric Terminal Tungsten Methylidyne Complex. *J. Am. Chem. Soc.* **2001,** *123* (21), 4992-5002.

22. Hejl, A.; Trnka, T. M.; Day, M. W.; Grubbs, R. H. Terminal ruthenium carbido complexes as σ-donor ligands. *Chem. Commun.* **2002,** (21), 2524-2525.

23. Carlson, R. G.; Gile, M. A.; Heppert, J. A.; Mason, M. H.; Powell, D. R.; Velde, D. V.; Vilain, J. M. The Metathesis-Facilitated Synthesis of Terminal Ruthenium Carbide Complexes: A Unique Carbon Atom Transfer Reaction. *J. Am. Chem. Soc.* **2002,** *124* (8), 1580-1581.

24. Stewart, M. H.; Johnson, M. J. A.; Kampf, J. W. Terminal Carbido Complexes of Osmium: Synthesis, Structure, and Reactivity Comparison to the Ruthenium Analogues. *Organometallics* **2007,** *26* (20), 5102-5110.

25. Buss, J. A.; Agapie, T. Four-electron deoxygenative reductive coupling of carbon monoxide at a single metal site. *Nature* **2016,** *529* (7584), 72-75.

26. Buss, J. A.; Agapie, T. Mechanism of Molybdenum-Mediated Carbon Monoxide Deoxygenation and Coupling: Mono- and Dicarbyne Complexes Precede C–O Bond Cleavage and C–C Bond Formation. *J. Am. Chem. Soc.* **2016,** *138* (50), 16466-16477.

27. Teets, T. S.; Labinger, J. A.; Bercaw, J. E. A Thermodynamic Analysis of Rhenium(I)–Formyl C–H Bond Formation via Base-Assisted Heterolytic H_2 Cleavage in the Secondary Coordination Sphere. *Organometallics* **2013,** *32* (19), 5530-5545.

28. Miller, A. J. M.; Labinger, J. A.; Bercaw, J. E. Homogeneous CO Hydrogenation: Dihydrogen Activation Involves a Frustrated Lewis Pair Instead of a Platinum Complex. *J. Am. Chem. Soc.* **2010,** *132* (10), 3301-3303.

29. Miller, A. J. M.; Labinger, J. A.; Bercaw, J. E. Reductive Coupling of Carbon Monoxide in a Rhenium Carbonyl Complex with Pendant Lewis Acids. *J. Am. Chem. Soc.* **2008,** *130* (36), 11874-11875.

30. Carbide **1** was synthesized cleanly in situ via deprotonation of P2Mo(CH)(CO)(Cl) **4** with benzyl potassium. For more details, see the Supporting Information.

31. Dwyer, D. J.; Somorjai, G. A. Hydrogenation of CO and CO_2 over iron foils: Correlations of rate, product distribution, and surface composition. *J. Catal.* **1978,** *52* (2), 291-301.

32. ^{13}C labeled complexes (originating from ^{13}CO, see ref. 25) were used throughout these studies, leveraging an advantageous spectroscopic handle for both Mo complex speciation and determining the nature of the CO-derived ligands. Solid-state structures and full characterization data were often pursued with unlabeled complexes after the initial reactivity trends had been mapped out.

33. Brar, A.; Unruh, D. K.; Aquino, A. J.; Krempner, C. Lewis acid base chemistry of Bestmann's ylide, Ph_3PCCO, and its bulkier analogue, $(cyclohexyl)_3PCCO$. . *Chem. Commun.* **2019,** *55* (24), 3513-3516.

34. Selected examples: (a) Lindner, E. New aspects of metal carbonyl ylide chemistry. *J. Organomet. Chem.* **1975,** *94* (2), 229-234. (b) Bertani, R.; Casarin, M.; Ganis, P.; Maccato, C.; Pandolfo, L.; Venzo, A.; Vittadini, A.; Zanotto, L. Organometallic Chemistry of Ph_3PCCO. Synthesis, Characterization, X-ray Structure Determination, and Density Functional Study of the First Stable Bis-η^1-ketenyl Complex, trans-$[PtCl_2\{\eta^1\text{-}C(PPh_3)CO\}_2]$. *Organometallics* **2000,** *19* (7), 1373-1383. (c) Alcarazo, M.; Lehmann, C. W.; Anoop, A.; Thiel, W.; Fürstner, A. Coordination chemistry at carbon. *Nature Chem.* **2009,** *1*, 295.

35. (a) List, A. K.; Hillhouse, G. L.; Rheingold, A. L. A carbon-carbon bond cleavage reaction of carbon suboxide at a metal center. Synthesis and structural characterization of $WCl_2(CO)(PMePh_2)_2\{C,C':\eta_2\text{-}C(O)CPMePh_2\}$. *J. Am. Chem. Soc.* **1988,** *110* (14), 4855-4856. (b) List, A. K.; Hillhouse, G. L.; Rheingold, A. L. Carbon suboxide as a C1 reagent. Sequential cleavage of CO from C_3O_2 at a metal center to give $WCl_2(CO)(PMePh_2)_2[C,C':\eta^2\text{-}C(O)CPMePh_2]$ and $WCl_2(CO)(PMePh_2)_2(CPMePh_2)$. *Organometallics* **1989,** *8* (8), 2010-2016.

36. Kreissl, F. R.; Friedrich, P.; Huttner, G. *p*-Tolylketenyl as Novel dihapto 3-Electron Ligand. *Angew. Chem. Int. Ed. Engl.* **1977,** *16* (2), 102-103.

37. Kreissl, F. R.; Frank, A.; Schubert, U.; Lindner, T. L.; Huttner, G. Carbonyl-η-cyclopentadienyl-(4-methylphenylketenyl)-bis (trimethylphosphane)tungsten—A Novel, Stable Transition Metal-Substituted Ketene. *Angew. Chem. Int. Ed. Engl.* **1976,** *15* (10), 632-633.

38. LaPointe, R. E.; Wolczanski, P. T.; Mitchell, J. F. Carbon monoxide cleavage by $(silox)_3Ta$ (silox = tert-Bu_3SiO-). *J. Am. Chem. Soc.* **1986,** *108* (20), 6382-6384.

39. Neithamer, D. R.; LaPointe, R. E.; Wheeler, R. A.; Richeson, D. S.; Van Duyne, G. D.; Wolczanski, P. T. Carbon monoxide cleavage by $(silox)_3Ta$ (silox = tert-Bu_3SiO-) physical, theoretical, and mechanistic investigations. *J. Am. Chem. Soc.* **1989,** *111* (25), 9056-9072.

40. Wolfgruber, M.; Kreissi, F. R. Übergangsmetalleten-Verbindungen: XXXI. Addition von Dimethyichlorphosphin an die Metall Kohlenstoff Dreifachbindung, eine neuartige CC-Kupplungsreaktion. *J. Organomet. Chem.* **1988,** *349* (1), C4-C6.

41. Valyaev, D. A.; Filippov, O. A.; Lugan, N.; Lavigne, G.; Ustynyuk, N. A. Umpolung of Methylenephosphonium Ions in Their Manganese Half-Sandwich Complexes and Application to the Synthesis of Chiral Phosphorus-Containing Ligand Scaffolds. *Angew. Chem. Int. Ed.* **2015,** *54* (21), 6315-6319.

42. Valyaev, D. A.; Utegenov, K. I.; Krivykh, V. V.; Willot, J.; Ustynyuk, N. A.; Lugan, N. Dual reactivity pattern of Mn(I) carbyne complexes $Cp(CO)_2Mn^+{\equiv}C\text{–}R$ (R = Ar, Alk) vs. dppm: Subtle balance between double intramolecular nucleophilic addition and nucleophilic addition followed by migratory CO insertion. *J. Organomet. Chem.* **2018,** *867*, 353-358.

43. A complementary strategy involves the addition of exogenous CO to a transition metal–ylide complex. See: (a)

Mao, W.; Wang, Y.; Xiang, L.; Peng, Q.; Leng, X.; Chen, Y., *Chem. Eur. J.* **2019,** *Early View*. (b) Liu, N.; Wang, A.; Sun, H.; Li, X., *Organometallics* **2010,** *29* (8), 1996-1996.

44. Greco, J. B.; Peters, J. C.; Baker, T. A.; Davis, W. M.; Cummins, C. C.; Wu, G. Atomic Carbon as a Terminal Ligand: Studies of a Carbidomolybdenum Anion Featuring Solid-State ^{13}C NMR Data and Proton-Transfer Self-Exchange Kinetics. *J. Am. Chem. Soc.* **2001,** *123* (21), 5003-5013.

45. Jamison, G. M.; Bruce, A. E.; White, P. S.; Templeton, J. L. Monomeric Group VI (M = molybdenum, tungsten) methylidyne complexes and their dimerization to nonclassical vinylidene-bridged $Tp'(CO)_2M(\mu\text{-}CCH_2)M(CO)_2Tp'$ products. *J. Am. Chem. Soc.* **1991,** *113* (13), 5057-5059.

46. Holmes, S. J.; Clark, D. N.; Turner, H. W.; Schrock, R. R. Multiple metal-carbon bonds. 26. α-Hydride elimination from methylene and neopentylidene ligands. Preparation and protonation of tungsten(IV) methylidyne and neopentylidyne complexes. *J. Am. Chem. Soc.* **1982,** *104* (23), 6322-6329.

47. Schrock, R. R.; Seidel, S. W.; Mösch-Zanetti, N. C.; Shih, K.-Y.; O'Donoghue, M. B.; Davis, W. M.; Reiff, W. M. Synthesis and Decomposition of Alkyl Complexes of Molybdenum(IV) That Contain a $[(Me_3SiNCH_2CH_2)_3N]_3$-Ligand. Direct Detection of α-Elimination Processes That Are More than Six Orders of Magnitude Faster than β-Elimination Processes. *J. Am. Chem. Soc.* **1997,** *119* (49), 11876-11893.

48. Kuiper, D. S.; Douthwaite, R. E.; Mayol, A.-R.; Wolczanski, P. T.; Lobkovsky, E. B.; Cundari, T. R.; Lam, O. P.; Meyer, K. Molybdenum and Tungsten Structural Differences are Dependent on $nd_{z^2}/(n + 1)s$ Mixing: Comparisons of $(silox)_3MX/R$ (M = Mo, W; silox = tBu_3SiO). *Inorg. Chem.* **2008,** *47* (16), 7139-7153.

49. Chisholm, M. H.; Folting, K.; Hoffman, D. M.; Huffman, J. C. Metal alkoxides: models for metal oxides. 4. Alkyne adducts of ditungsten hexaalkoxides and evidence for an equilibrium between dimetallatetrahedrane and methylidynemetal complexes: $W_2(\mu\text{-}C_2H_2)$ $2W{\equiv}CH$. *J. Am. Chem. Soc.* **1984,** *106* (22), 6794-6805.

50. Kurogi, T.; Carroll, P. J.; Mindiola, D. J. A Terminally Bound Niobium Methylidyne. *J. Am. Chem. Soc.* **2016,** *138* (13), 4306-4309.

51. Hill, A. F.; Ward, J. S.; Xiong, Y. Synthesis of a Stable Methylidyne Complex. *Organometallics* **2015,** *34* (20), 5057-5064.

52. Casey, C. P.; Fagan, P. J.; Miles, W. H. Synthesis and interconversions of dinuclear iron complexes with μ-methyl, μ-methylene, and μ-methylidyne ligands. *J. Am. Chem. Soc.* **1982,** *104* (4), 1134-1136.

53. Gunnoe, T. B.; Surgan, M.; White, P. S.; Templeton, J. L.; Casarrubios, L. Synthesis and Reactivity of Tungsten(II) Methylene Complexes. *Organometallics* **1997,** *16* (22), 4865-4874.

54. Churchill, M. R.; Wasserman, H. J. Crystal and molecular structure of $[W(CH_2PMe_3)(CO)_2Cl(PMe_3)_3][CF_3SO_3]$, a seven-coordinate tungsten(II) complex produced by transfer of a trimethylphosphine to the $W{=}CH_2$ system. *Inorg. Chem.* **1982,** *21* (11), 3913-3916.

55. Moss, J. R.; Niven, M. L.; Stretch, P. M. Haloalkyl complexes of the transition metals. Part 5. The synthesis and reactions of some new pentamethylcyclopentadienyl halomethyl and methoxymethyl complexes of molybdenum(II) and tungsten(II) and the X-ray crystal structure of the cationic ylide complex$[\eta\text{-}C_5Me_5W(CO)_3CH_2PPh_3]I$. *Inorg. Chim. Acta* **1986,** *119* (2), 177-186.

56. For reference, the $^1J(P,C_{CH2})$ coupling constant in CH_2PMe_3 is 90(3) Hz (see ref. 24).

57. Jolly, P. W., 37.3 - Lewis-base Nickel Carbonyl Complexes. In *Comprehensive Organometallic Chemistry*, Wilkinson, G.; Stone, F. G. A.; Abel, E. W., Eds. Pergamon: Oxford, 1982; pp 15-36.

58. Bodnar, T. W.; Cutler, A. R. Formation of a stable $(\eta^2\text{-}C,C)$ ketene compound dicarbonyl(cyclopentadienyl)keteneiron hexafluorophosphate $[(C_5H_5)Fe(CO)_2(CH_2CO)^+ PF_6^-]$ by carbonylation of an iron-methylidene complex. A novel entry into carbonyl-derived C_2 chemistry. *J. Am. Chem. Soc.* **1983,** *105* (18), 5926-5928.

59. Buss, J. A.; Edouard, G. A.; Cheng, C.; Shi, J.; Agapie, T. Molybdenum Catalyzed Ammonia Borane Dehydrogenation: Oxidation State Specific Mechanisms. *J. Am. Chem. Soc.* **2014,** *136* (32), 11272-11275.

60. Hommeltoft, S. I.; Baird, M. C. .beta.-Elimination from a metal acetyl compound to form ketene and a metal hydride. *J. Am. Chem. Soc.* **1985,** *107* (8), 2548-2549.

61. Free trimethylsilyl ketene has ^{13}C NMR chemical shifts at 179.2 and -0.1 ppm for C_a and C_b, respectively. These peaks do not match those observed and we attribute the difference to coordination of BEt_3. The ^{13}C chemical shifts of ketenes vary dramatically based on the electronic character at carbon (*ca.* -20 to 50 ppm $[C_b]$ and 165 to 205 ppm $[C_a]$); the experimentally observed resonances fall within this range and have $^1J(C,C)$ couplings consistent with the ketene assignment. For more details refer to: Seikaly, H. R.; Tidwell, T. T. *Tetrahedron* **1986**, *42*, 2587.

62. Seikaly, H. R.; Tidwell, T. T. Addition reactions of ketenes. *Tetrahedron* **1986,** *42* (10), 2587-2613.

63. Lin, Y. C.; Calabrese, J. C.; Wreford, S. S. Preparation and reactivity of a dimeric ruthenium μ-methylene complex with no metal-metal bond: crystal and molecular structure of $[(\eta^5\text{-}C_5H_5)Ru(CO)_2]_2(\mu\text{-}CH_2)$. *J. Am. Chem. Soc.* **1983,** *105* (6), 1679-1680.

64. Herrmann, W. A.; Plank, J. High-Pressure Carbonylation of Metal-Coordinated Carbenes and Hydrogenolysis of the Ketene Complexes. *Angew. Chem. Int. Ed. Engl.* **1978,** *17* (7), 525-526.

65. Miyashita, A.; Shitara, H.; Nohira, H. Preparation and properties of platinum ketene complexes. Facile carbon-carbon bond cleavage of coordinated ketene. *Organometallics* **1985,** *4* (8), 1463-1464.

66. Grotjahn, D. B.; Bikzhanova, G. A.; Collins, L. S. B.; Concolino, T.; Lam, K.-C.; Rheingold, A. L. Controlled, Reversible Conversion of a Ketene Ligand to Carbene and CO Ligands on a Single Metal Center. *J. Am. Chem. Soc.* **2000,** *122* (21), 5222-5223.

67. Barger, P. T.; Santarsiero, B. D.; Armantrout, J.; Bercaw, J. E. Carbene complexes of zirconium. Synthesis, structure, and reactivity with carbon monoxide to afford coordinated ketene. *J. Am. Chem. Soc.* **1984,** *106* (18), 5178-5186.

68. Herrmann, W. A.; Gimeno, J.; Weichmann, J.; Ziegler, M. L.; Balbach, B. Komplexchemie reaktiver organischer verbindungen: XXXVII. Metallinduzierter abbau eines σ,π-koordinierten ketens in ein π-allyl/σ-aryl/π-olefin-system. *J. Organomet. Chem.* **1981,** *213* (2), C26-C30.

69. Kurogi, T.; Ishida, Y.; Hatanaka, T.; Kawaguchi, H. Reduction of carbon monoxide by a tetrakis(aryloxide)diniobium complex having four bridging hydrides. *Dalton Transactions* **2013,** *42* (21), 7510-7513.

70. Matsuo, T.; Kawaguchi, H. A Synthetic Cycle for H_2/CO Activation and Allene Synthesis Using Recyclable Zirconium Complexes. *J. Am. Chem. Soc.* **2005,** *127* (49), 17198-17199.

71. Morrison, E. D.; Steinmetz, G. R.; Geoffroy, G. L.; Fultz, W. C.; Rheingold, A. L. Interconversion of methylene and ketene ligands on a triosmium cluster. Crystal and molecular structure of the ketene complex dodecacarbonyl[^{2}(C,C)-μ-ketene]triosmium, [$Os_3(CO)_{12}$[η^2(C,C)-μ-CH_2CO]]. *J. Am. Chem. Soc.* **1983,** *105* (12), 4104-4105.

72. Morrison, E. D.; Steinmetz, G. R.; Geoffroy, G. L.; Fultz, W. C.; Rheingold, A. L. Trinuclear osmium clusters as models for intermediates in carbon monoxide reduction chemistry. 2. Conversion of a methylene into a ketene ligand on a triosmium cluster face. *J. Am. Chem. Soc.* **1984,** *106* (17), 4783-4789.

73. Straus, D. A.; Grubbs, R. H. Preparation and reaction of metal-ketene complexes of zirconium and titanium. *J. Am. Chem. Soc.* **1982,** *104* (20), 5499-5500.

74. Asdar, A.; Lapinte, C.; Toupet, L. Synthesis and electrophilic properties of neutral molybdenum formyl complexes Mo(C_5Me_5)$(CO)_2(PR_3)$CHO: access to secondary heterocarbene compounds. *Organometallics* **1989,** *8* (11), 2708-2717.

75. Tam, W.; Lin, G.-Y.; Gladysz, J. A. Syntheses of kinetically unstable neutral formyl complexes via Li(C_2H_5)$_3$BH and "transformylation" reactions of metal carbonyl cations. *Organometallics* **1982,** *1* (3), 525-529.

76. Tam, W.; Wong, W.-K.; Gladysz, J. A. Neutral metal formyl complexes: generation, reactivity, and models for Fischer-Tropsch catalyst intermediates. *J. Am. Chem. Soc.* **1979,** *101* (6), 1589-1591.

77. Gibson, D. H.; Owens, K.; Mandal, S. K.; Sattich, W. E.; Franco, J. O. Synthesis and thermolysis of neutral metal formyl complexes of molybdenum, tungsten, manganese, and rhenium. *Organometallics* **1989,** *8* (2), 498-505.

78. Elowe, P. R.; West, N. M.; Labinger, J. A.; Bercaw, J. E. Transformations of Group 7 Carbonyl Complexes: Possible Intermediates in a Homogeneous Syngas Conversion Scheme. *Organometallics* **2009,** *28* (21), 6218-6227.

79. Butts, S. B.; Holt, E. M.; Strauss, S. H.; Alcock, N. W.; Stimson, R. E.; Shriver, D. F. Kinetic and thermodynamic control of the methyl migration (carbon monoxide insertion) reaction by strong Lewis acids. *J. Am. Chem. Soc.* **1979,** *101* (19), 5864-5866.

80. Richmond, T. G.; Basolo, F.; Shriver, D. F. Bifunctional activation of coordinated carbon monoxide: a kinetic study of Lewis acid induced alkyl migration. *Inorg. Chem.* **1982,** *21* (3), 1272-1273.

81. Fischer, E. O.; Frank, A. Übergangsmetall-Carbin-Komplexe, XLIII: Reduktion einer Metall-Kohlenstoff-Dreifachbindung. *Chem. Ber.* **1978,** *111* (11), 3740-3744.

82. Fischer, E. O.; Clough, R. L.; Besl, G.; Kreissl, F. R. Dimethylcarbene- and Methylphenylcarbenedicarbonyl(η-cyclopentadienyl)manganese. *Angew. Chem. Int. Ed. Engl.* **1976,** *15* (9), 543-544.

83. Bruce, A. E.; Gamble, A. S.; Tonker, T. L.; Templeton, J. L. Cationic phosphonium carbyne and bis(phosphonium) carbene tungsten complexes: [Tp'$(OC)_2$WC$(PMe_3)_n$][PF_6] (n = 1, 2). *Organometallics* **1987,** *6* (6), 1350-1352.

84. Buss, J. A.; VanderVelde, D. G.; Agapie, T. Lewis Acid Enhancement of Proton Induced CO2 Cleavage: Bond Weakening and Ligand Residence Time Effects. *J. Am. Chem. Soc.* **2018,** *140* (32), 10121-10125.

85. Kandler, H.; Bidell, W.; Jänicke, M.; Knickmeier, M.; Veghini, D.; Berke, H. Functionalized Iron Ketene Complexes from Carbonyl Coupling Reactions. *Organometallics* **1998,** *17* (5), 960-971.

86. Black, T. H.; Farrell, J. R.; Probst, D. A.; Zotz, M. C. A high-yielding, reproducible synthesis of trimethylsilylketene. *Synth. Commun.* **2002,** *32* (13), 2083-2088.

87. Staudaher, N. D.; Arif, A. M.; Louie, J. Synergy between Experimental and Computational Chemistry Reveals the Mechanism of Decomposition of Nickel–Ketene Complexes. *J. Am. Chem. Soc.* **2016,** *138* (42), 14083-14091.

88. Curley, J. J.; Kitiachvili, K. D.; Waterman, R.; Hillhouse, G. L. Sequential Insertion Reactions of Carbon Monoxide and Ethylene into the Ni–C Bond of a Cationic Nickel(II) Alkyl Complex. *Organometallics* **2009,** *28* (8), 2568-2571.

89. Ho, S. C. H.; Straus, D. A.; Armantrout, J.; Schaefer, W. P.; Grubbs, R. H. Structure and reactivity of the zirconaenolate anion[Cp_2Zr(C,O-η^2-$OCCH_2$)CH_3]Na•2THF. Synthesis of homo- and heterobinuclear ketene complexes. *J. Am. Chem. Soc.* **1984,** *106* (7), 2210-2211.

90. Bleuel, E.; Laubender, M.; Weberndörfer, B.; Werner, H. The First Example of Linkage-Isomeric Ketene Metal Complexes. *Angew. Chem. Int. Ed.* **1999,** *38* (1-2), 156-159.

91. Grotjahn, D. B.; Lo, H. C. Fragmentation of 2-Pyridyl Esters Gives both .^{2}(C,O)- and ^{2}(C,C)-Bound Ketene Ligands on ClIr[P(i-Pr)$_3$]$_2$. *Organometallics* **1995,** *14* (12), 5463-5465.

92. Grotjahn, D. B.; Collins, L. S. B.; Wolpert, M.; Bikzhanova, G. A.; Lo, H. C.; Combs, D.; Hubbard, J. L. First Direct Structural Comparison of Complexes of the Same Metal Fragment to Ketenes in Both C,C- and C,O-Bonding Modes. *J. Am. Chem. Soc.* **2001,** *123* (34), 8260-8270.

93. Zhao, Y.; Truhlar, D. G. The M06 suite of density functionals for main group thermochemistry, thermochemical kinetics, noncovalent interactions, excited states, and transition elements: two new functionals and systematic testing of four M06-class functionals and 12 other functionals. *Theor. Chem. Acc.* **2008,** *120* (1), 215-241.

94. Anslyn, E. V.; Goddard, W. A. Structures and reactivity of neutral and cationic molybdenum methylidene complexes. *Organometallics* **1989,** *8* (6), 1550-1558.

95. Some degree of O–borane interaction is apparently also present in methylidene **5**, as judged by parallel experiments with BPh_3 (described below), in which the ^{31}P chemical shift for **5** is detected slightly upfield at 49.4 ppm (cf. 52.1 ppm in the reaction with BEt_3). No such change in chemical shift was detected for **6** in these two reactions,

however; nor was it detected for bound ketene complex **11** generated in the presence or absence of BEt_3. We conclude that O–borane interactions are likely important for stabilizing reaction intermediates during C–C coupling, but that they are not ubiquitously present in the ground-state structures.

96. Pérez-Gallent, E.; Marcandalli, G.; Figueiredo, M. C.; Calle-Vallejo, F.; Koper, M. T. M. Structure- and Potential-Dependent Cation Effects on CO Reduction at Copper Single-Crystal Electrodes. *J. Am. Chem. Soc.* **2017,** *139* (45), 16412-16419.

97. Paik, W.; Andersen, T. N.; Eyring, H. Kinetic studies of the electrolytic reduction of carbon dioxide on the mercury electrode. *Electrochim. Acta* **1969,** *14* (12), 1217-1232.

98. Garrido, G.; Koort, E.; Ràfols, C.; Bosch, E.; Rodima, T.; Leito, I.; Rosés, M. Acid–Base Equilibria in Nonpolar Media. Absolute pKa Scale of Bases in Tetrahydrofuran. *J. Org. Chem.* **2006,** *71* (24), 9062-9067.

99. Heiden, Z. M.; Lathem, A. P. Establishing the Hydride Donor Abilities of Main Group Hydrides. *Organometallics* **2015,** *34* (10), 1818-1827.

100. Curtis, C. J.; Miedaner, A.; Ellis, W. W.; DuBois, D. L. Measurement of the Hydride Donor Abilities of $[HM(diphosphine)_2]^+$Complexes (M = Ni, Pt) by Heterolytic Activation of Hydrogen. *J. Am. Chem. Soc.* **2002,** *124* (9), 1918-1925.

101. The effective pK_a of methylidyne **4** is designated as pK_a(Cl) to indicate that the observed reactivity reflects both the free energy of proton transfer (pK_a) and the free energy of chloride binding to Mo.

102. Saame, J.; Rodima, T.; Tshepelevitsh, S.; Kütt, A.; Kaljurand, I.; Haljasorg, T.; Koppel, I. A.; Leito, I. Experimental Basicities of Superbasic Phosphonium Ylides and Phosphazenes. *J. Org. Chem.* **2016,** *81* (17), 7349-7361.

103. Because of the limited availability of hydricity values reported in THF, and the reactivity of Mo-P2 complexes in MeCN, we rely on the hydricity values in MeCN, but use the pK_a values determined in THF, to get an approximation of the Gibbs free energy of H_2 addition to **1**. To correct for these solvent effects, we used Morris' method to estimate a lower bound for the pK_a of methylidyne **4** in MeCN from the experimentally determined pK_a in THF. Even with this correction factor applied, the addition of H_2 to **1** remains thermoneutral ($pK_a^{MeCN} > 28$; $\Delta G < 1.5$ kcal / mol). See: Morris, R. H. Estimating the Acidity of Transition Metal Hydride and Dihydrogen Complexes by Adding Ligand Acidity Constants. *J. Am. Chem. Soc.* **2014,** *136* (5), 1948-1959.

104. Soluble KCl is carried forward from the *in situ* synthesis of **1**, as evidenced by experiments in which **1** was treated with acids bearing $BAr^F{}_4$ counterions, and *chloride*-bound methylidynes **4**/**4'** were generated as the primary products (see the SI). Even so, no reaction was observed between carbide **1** and H_2.

105. Davies, H. M. L.; Manning, J. R. Catalytic C–H functionalization by metal carbenoid and nitrenoid insertion. *Nature* **2008,** *451*, 417.

106. Park, Y.; Kim, Y.; Chang, S. Transition Metal-Catalyzed C–H Amination: Scope, Mechanism, and Applications. *Chem. Rev.* **2017,** *117* (13), 9247-9301.

107. Chu, J. C. K.; Rovis, T. Complementary Strategies for Directed C(sp^3)–H Functionalization: A Comparison of Transition-Metal-Catalyzed Activation, Hydrogen Atom Transfer, and Carbene/Nitrene Transfer. *Angew. Chem. Int. Ed.* **2018,** *57* (1), 62-101.

Insert Table of Contents artwork here

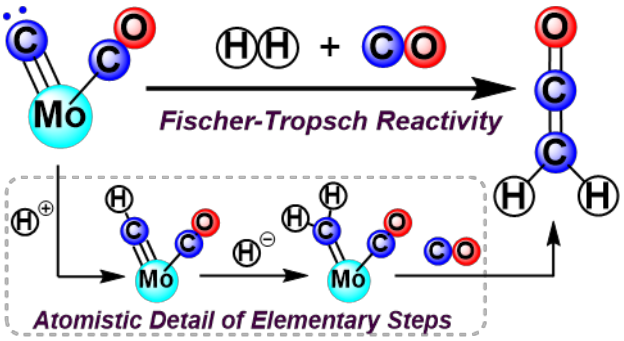

Insert Table of Contents artwork here